2018

Modification of Electrical Properties of Silver Nanoparticle

Markus Diantoro, *State University of Malang*
Thathit Suprayogi, *State University of Malang*
Ulwiyatus Sa'adah, *State University of Malang*
Nandang Mufti, *State University of Malang*
Abdulloh Fuad, *State University of Malang*, et al.

Chapter 12

Modification of Electrical Properties of Silver Nanoparticle

Markus Diantoro, Thathit Suprayogi, Ulwiyatus Sa'adah, Nandang Mufti, Abdulloh Fuad, Arif Hidayat and Hadi Nur

Additional information is available at the end of the chapter

http://dx.doi.org/10.5772/intechopen.75682

Abstract

This chapter focuses on the synthesis of silver nanoparticles (AgNPs), AgNP composites, and its role in the structure and electrical properties modification. The research and its various applications of nanoparticles are interesting among others. Silver nanoparticles (AgNPs) are now becoming to take an essential role in the diverse field of application. Establishing the simple and inexpensive of AgNPs is greatly required, since it will also influence it used. Many different methods to obtain AgNPs have been reported. The inducing AgNPs on a various number of other materials has been investigating. We report a brief review of simple AgNP fabrication method at different MSA, PEG, and ultrasonic irradiations regarding its structure and conductivity. We also report the influence of AgNPs on the electrical conductivity of conducting polymers, i.e., PANI, flavonoids of *Jatropha multifida* L. (JML) and *Pterocarpus indicus* W. (PIW). It is found that in general, the increase of AgNP concentration gives rise to increase of its electrical conductivity. The conductivity of the AgNPs doped of polymers does not directly reflect by its crystallinity or crystal size. Some exciting aspect of crystal structure and its conductivity are discussed.

Keywords: silver nanoparticles, mercaptosuccinic acid, *Pterocarpus indicus* W., *Jatropha multifida* L., polyaniline, conductivity

1. Introduction

The silver nanoparticle research continues to grow, drawing the attention of researchers. It is known that silver has very high electrical conductivity [1, 2]. Silver has been widely used as a

conductor wire in circuits that require low dissipation, and high conductivity [3, 4]. Silver paste has also been widely used as a paste conductor [5–7]. The use of silver paste has been extensively utilized mainly in the bulk conductivity characterization of bulk semiconductor materials or four-point probe method films. In the field of superconductors, silver has a dominant role as a sheath [8–12]. Silver has also been used in various industries and health fields. Silver is known to have antibacterial properties [13–16], as a catalyst [17–20], and it shows stable to the environment [21] and has been utilized as a significant component of water treatment.

Various methods of synthesis have been developed to produce silver in the order of nanometers. Synthesis of silver nanoparticle is commonly known to control the shape and size. Among these methods are ball milling method [22], precipitation [23], polyol method [24], and several other methods to produce silver nanoparticle [3, 25–28].

Nanostructure engineering has been performed to produce the expected properties. Nanofluid Ag-ZnO has been successfully synthesized to determine the behavior of thermal conductivity at various fractions [29]. Silver nanoparticles dotted on the external walls of multi-walled carbon nanotubes (MWCNTs) were prepared by an aldehyde reduction process in supercritical carbon dioxide ($SCCO_2$) fluid. The friction reduced about 30% [30]. Modification of nanostructure Ag into nanowire also improves physical performance such as electrical conductivity and power transfer [31]. Further engineering in the form of silver nanocage has reported. The nanocages exhibited unique and attractive characteristics for metal catalytic systems, thus offering the scope for new development as heterogeneous catalysts [32]. The aqueous persistence performance of Ag nanocolloids particles has been studied in depth in various environments [33]. Silver nanoparticles capped with Oleylamine (AgNPs/OLA) and its application in conductive ink for the electroanalytical application has been reported in [34].

Some of those examples show that silver nanoscale research and application are of concern to researchers. Due to the broad scope of the study of silver nanoparticles, we have limited this article to the synthesis of nanoparticles by simple methods, particle nanoparticle effects on structures, and electrical properties in polymers such as polyaniline, and some organic polymers such as *Pterocarpus indicus* Willd (PIW) and *Jatropha multifida* Linn (JML).

2. Materials and method

2.1. Synthesis of silver nanoparticle with various MSA

Basic of experimental method used in the current work was a chemical reduction from the silver nitrate salt of $AgNO_3$. The silver nitrate ($AgNO_3$) dissolves into a positive ion (Ag^+) and negative ion (NO_3^-). From the process, we could obtain solid silver grain due to the ions experience a reduction process by accepting electrons from a donor. After forming the silver nucleus, a crystal growth continues at the relatively short time. By this way, a crystal of nanosize obtained. This nanoparticle fabrication and other similar synthesize are known as bottom-up technic.

The raw materials used are silver nitrate $AgNO_3$, sodium borohydride $NaBH_4$ as a reductor, and mercaptosuccinic acid (MSA) as a stabilizer. Conventional solvents which normally used

are aquades and methanol. A series of MSA, namely 0.03, 0.06, 0.12, and 0.15 M, was dissolved in methanol of 400 mL, then stirred rigorously using magnetic stirrer in an ice bath. Into the solution, add the second solution, i.e., silver nitrate about 340 mg to 6.792 mL aquades. While the mixture of both solutions is being stirred, sodium borohydride of 756.6 mg in 100 mL aquades drops small wisely. After adding the second solvent, the clear MSA solution changed into an amber one. Further, by adding the third solution, the mixture solution transforms into black-brownish. The final solution has then employed a stirring for 30 min at 500 rpm and maintained at a temperature of 5–10°C. The obtained particles then rinse using methanol on Whatman filter. The latter step was conducted several times to ensure the only silver particle remains. The collected material was then exposed to 80°C yielding silver nanopowder.

2.2. Synthesis of PANI-AgNP film

Two series of silver-doped PANI-AgNPs/Ni and ultrasonic irradiation time films have been prepared using spin-coating method. Each series was provided five samples. The basic configuration of PANI-EB and PANI-ES were synthesized following the procedure of previous report [7]. The solutions of PANI-Ag had been prepared with synthesizing PANI-EB from aniline using the chemical oxidizing method. About 1.82 mL aniline (0.1 M) was dissolved into 50 mL HCl (0.2 M) liquid for about 1 h. Along with this, a solution of 5.71 g $(NH_4)_2S_2O_8$ (0.1 M) in 50 mL aquadest was also prepared at the same time. After 1 h, those two solutions were mixed and stirred a while, then exposed at room temperature for about 24 h for polymerization. The precipitated material was filtered using Whatman filter paper, then washed using deionized water and aquades until clear liquids are observed. The obtained precipitated materials are then mixed and homogenized using magnetic stirrer in NH_4OH (0.5 M) for 4 h, and then let them rest for about 24 h and washed using aquades to obtain a blue PANI-EB. The powder of PANI-EB can be obtained after annealing the material for 5 h at 80°C. PANI-EB then mixed with camphor sulfonic acid (CSA) and then mixed with $AgNO_3$ solution in chloroform and employing ultrasonic irradiation for various irradiation times. The obtained solution was filtered to obtain a PANI-Ag solution for deposition on nickel substrate using spin-coating method. A different series of various $AgNO_3$ PANI doped of 0.1, 0.2, 0.3, 0.4, and 0.5 M was also prepared in the same manner. The films have been deposited onto 1 × 1 cm^2 Ni substrate using spin-coating method at 1000 rpm for 1 min. The obtained films were then annealed at 100°C for 1 min.

2.3. Synthesis of flavonoids' JML-AgNP and PIW-AgNP films

Samples were prepared in several stages. The initial step was the extraction of *Pterocarpus indicus* Willd (PIW) by preparing 800 g of *Pterocarpus indicus* Willd leaf powder mixed with 3 L methanol p.a. in a large bottle, and then the mixture was shaken and awaited for 1 week. After that, it was filtered using a Buckner funnel under pressure with Whatman's filter paper 01. The obtained slurry materials were evaporated using a rotary evaporator to get a rough methanol extract. About 25 g of methanol extract was introduced into the separating funnel, in which the mixture was manually shaken with 50 mL of n-hexane solvent for 30 min. Once separated, the two steps of this process are repeated using 50 mL n-hexane. The hexane phase in the treatment is separated, and the sum of the second procedure is combined and evaporated to obtain a crude hexane extract. The general process is applied to obtain extracts of

chloroform (100 mL), ethyl acetate (100 mL), and butanol (100 mL), respectively. In this way, flavonoid type quercetin can be achieved.

A similar way was performed to obtain a flavonoid extract of *Jatropha multifida* L. (JML) with a little more straightforward. The first step is extracting flavonoid using the wet method. Five grams of the liquid latex of JML, which was taken from wounded stem, was first heated on a glass plate to remove water. The water-free condensed latex was then solved into 10 mL of 80% methanol and homogenized for 30 min using magnetic stirrer while heating. In addition, it was also implemented to ultrasonic irradiation for 60 min, and let them to precipitate for 24 h. The mixture was then separated using a Whatman filter paper and dried up to evaporate the solvent to obtain flavonoid extract powder. The flavonoids of PIW can be prepared in a similar way using the extracted latex of the wounded stem.

To fabricate a thin film of AgNP-doped flavonoid, the mixture should be transformed into the liquid phase. In this case, two solutions were first prepared separately. The first solution was obtained from 0.1 M $AgNO_3$, which was dissolved in acetone. A relatively fine-ground camphor sulfonic acid (CSA) was mixed with the flavonoid extract PIW. The two solutions were then incorporated into a glass beaker and then stirred. The process proceeds until a homogenous mixture was obtained. To promote smaller size of silver ion as well as flavonoid incorporation in the homogenous mixture, we employed ultrasonic irradiation for 60 min. To achieve different AgNP-doped flavonoids/Ni films, the process has been repeated with a different $AgNO_3$ concentration of solutions. By following the preparation of JML-AgNP/Ni films, the flavonoid's PIW-AgNP/Ni films were also prepared in five different molar ratios of silver nitrate. The fabrication of those two nanosilver-doped films has been prepared using spin-coating method on nickel substrates of 1 × 1 cm^2 with 1500 rpm speed for 60 s. Each of the resulted film then follows annealing for repeating the process for concentrations of 0.2, 0.3, 0.4, and 0.5 M. The films finally annealed at 50°C for 5 min. Then those two series films were characterized using X-RD using Cu-Kα, FTIR, and four-probe electrical conductivity measurements.

3. Results and discussion

3.1. The influence of MSA on AgNP structures

Except for $NaBH_4$ for reducing agent, to synthesize nanometallic state, MSA is used as a reducing agent that also acts as a stabilizer agent of Ag^+. The synthetic silver nanoparticles are more stable and not easily oxidized. In addition, MSA also affects the size of the resulting silver nanocrystals. **Figure 1** shows the TEM results of spherical silver on the nanometer scale. The particle size of the TEM shows a yield of about 30 nm.

The TEM diffraction pattern of the sample was reported in our previous work [35]. It is shown that the sample is polycrystalline, which is indicated by the clear spots together with accompanying weak rings also reported by Majeed [36].

The X-ray diffraction pattern of obtained samples is displayed in **Figure 2**. Several identified peaks of intensity I-2θ are 38.10, 44.29, 64.43, 77.37, and 81.52°, associated to Bragg's planes

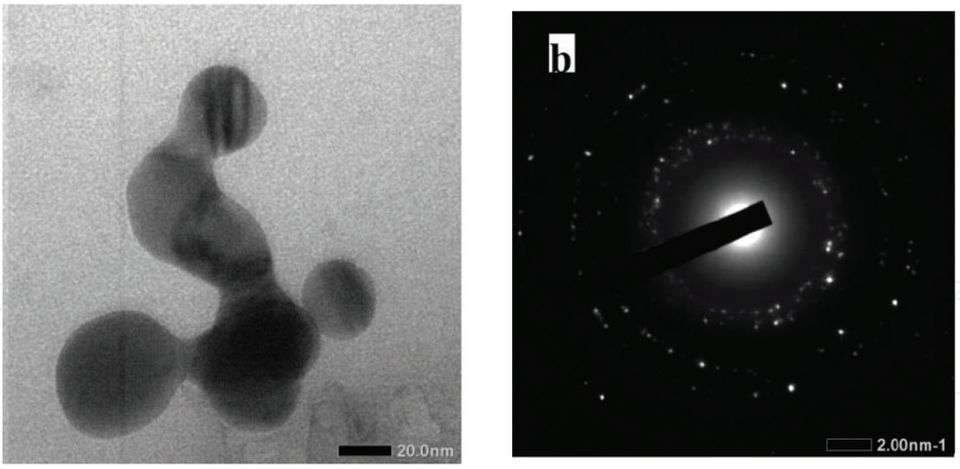

Figure 1. TEM image of silver nanoparticles and associated diffraction [35].

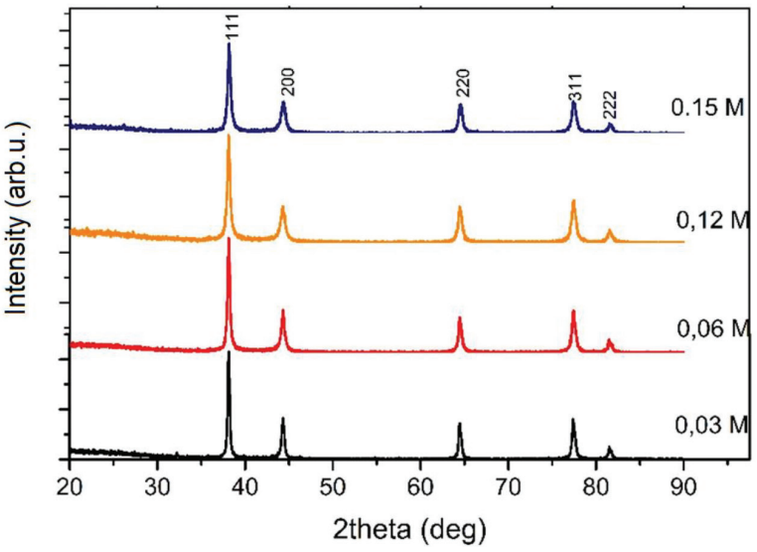

Figure 2. XRD pattern of AgNPs at various MSA concentration.

of (111), (200), (220), (311), and (222), respectively. There is apparently no other peaks, except the silver crystal peaks. All of the peaks shown in **Figure 2** can readily fit in a model of FCC structures, as also reported previously [37] for various PEG [23], for the different surfactant, and [38] for urea, PVP, and dextrose. Further refined to the lattice parameter gives rise to a = 4.0876 Å. This result insignificantly differs from the model of a = 4.0872 Å [36]. Detailed investigation to the same peak positions 2θ of all the diffraction patterns, even the peaks are not distinguished, it looks that the higher the fraction of MSA the broader the peaks. Broadening of diffraction peaks β, measured as FWHM, may show smaller crystal size (L) according to Scherrer's equation (Eq. (1)). Since crystal dimension L is just inversely proportional to its broadness of the peaks β.

$$L = \frac{K\lambda}{\beta \cos\theta} \tag{1}$$

It is also possible that one found different values of L from the same pattern. The origin of the discrepancies is mostly due to the K_α splitting, selecting the peaks, and fitting method of calculating β.

Based on the result of XRD as shown in **Figure 2**, the crystal size was calculated using Eq. (1). It shows that the size is in the range of 20–30 nm, which decreases with increasing concentration of MSA, as shown in **Figure 3**.

Of the two characterization analyses between TEM and XRD showed the size of the crystal is somewhat different results. The problems of crystal size calculation obtained from TEM, XRD, and/or probably SEM characterization is discussed in our work [35]. The crystal size obtained from XRD pattern calculation may be smaller than that derived from TEM. The discrepancy mostly not only originated from the di erent method of both types of equipment, but also due to the choosing peaks, implementing units of β and θ, as well as using the range of K in Eq. (1). The smaller diffraction angle we choose, the bigger the size we obtain. When the higher shape constant of K in the Scherrer formula, we may also get the bigger size. Sometime β is taken using degrees instead of radians. The crystal size calculation using a more compact software such as GSAS [39] or Fullprof [40]. In such software, they use the more rigid equation in Rietveld analyses with different compared to Eq. (1). The crystal size under GSAS or Fullprof is more comprehensive since they involve the strains, various profile functions as well as the anisotropy, or the crystal. The result of the crystal size obtained from the method is also slightly different from the manual using Scherrer equation. An example of manual crystal size calculation using a more complex equation is reported by Khan et al. [36]. It looks that there is a discrepancy of AgNP crystal size obtained by Scherrer and obtained from HRTEM. The average crystal size obtained by HRTEM shows a much bigger than that of using Scherrer equation. This result is similar to the work of Diantoro et al. [35].

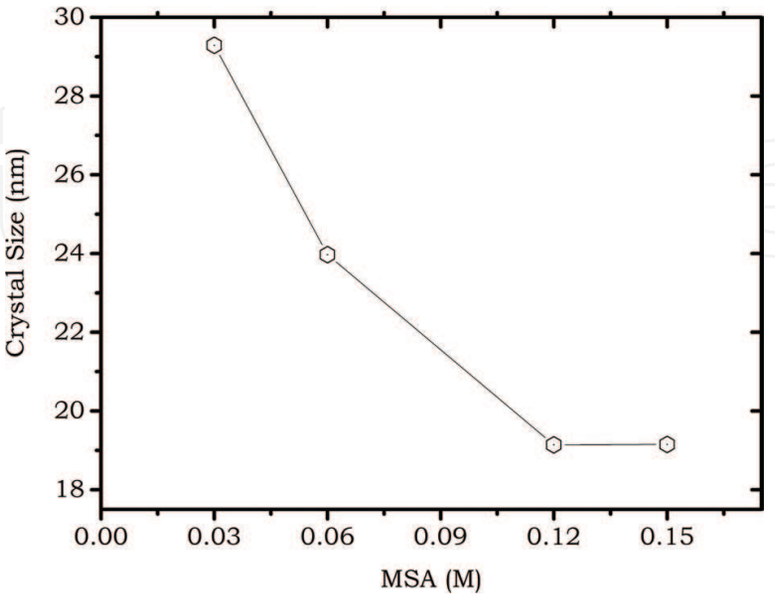

Figure 3. The influence of MSA concentration on AgNP crystal size.

Another capping agent such as polyethylene glycol (PEG) will be discussed briefly. We have obtained several AgNP samples which were prepared under the influence of PEG. The results are displayed in **Figure 4**.

Figure 4 shows the result of AgNP crystal size with increasing of PEG concentration. The silver crystal size lies around 12–24 nm. Based on **Figure 4**, it is seen that excluding of 0.075 M, increasing PEG concentration slightly decrease the crystals size. It could be indicated that PEG plays a role in controlling the crystal size. The researcher also uses PEG as a template for synthesizing nanoparticles [37]. One purpose of the use of PEG as a template or as a capping agent is not only to control the size, but also the distribution [41]. The effect of PVP repeating unit to the obtained crystal size of AgNPs was reported [18]. Many other solvents have been used for the synthesis of various size and shape of AgNPs, such as PEG [42], citrate [33, 43], and MSA [35].

3.2. The influence of AgNPs on crystal size and conductivity of PANI

It is shown that the size and shape of particles are affected by its physical properties [31, 32]. At the nanometer scale, the properties or characteristics of silver will change its electrical properties. Therefore, in the exploration of organic materials for electronics, silver nanoparticles can be incorporated with various conductive polymers such as PANI, JML, and PIW. The three polymers are conductive polymers with electric charge mechanisms of single- and double-conjugated bond hopping in the polymer. Although they said to be a conductive polymer, the pristine one is in the semiconductor range. So researcher expects that by controlling the metallic or oxidic nanoparticles may influence the electrical properties. In this report, we focus on the modification of the electrical conductivity. The following shows the effect of AgNP concentration on the electrical conductivity of PANI film as indicated in **Figure 5**.

The PANI composite with AgNPs indicates an increase in electrical conductivity by increasing the concentration of AgNPs used, as shown in **Figure 5**. The increased electrical conductivity of PANI is due to the increased electrical mobility derived from AgNPs in the compound. This

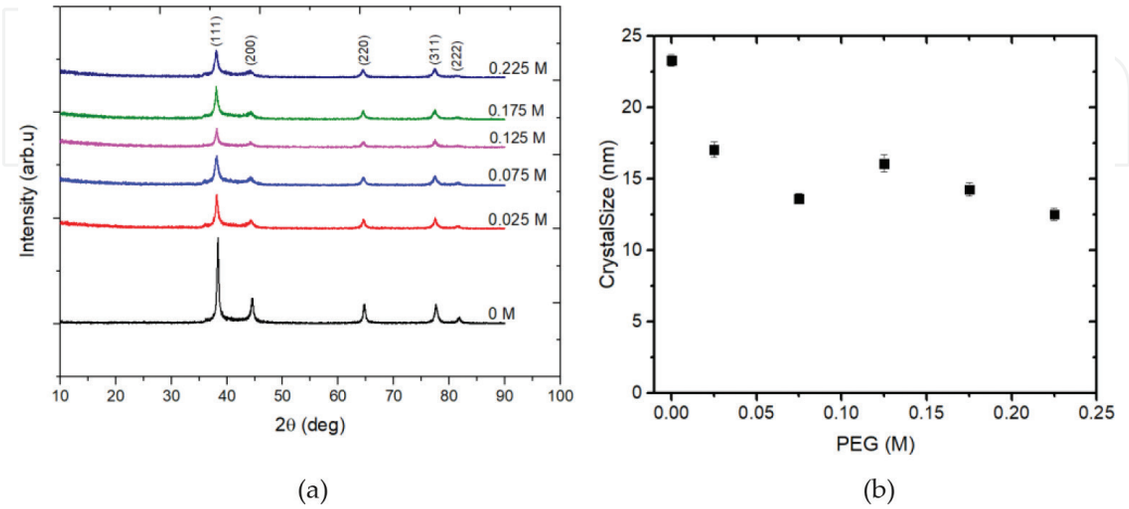

(a) (b)

Figure 4. The influence of PEG template (a) XRD and (b) crystal size.

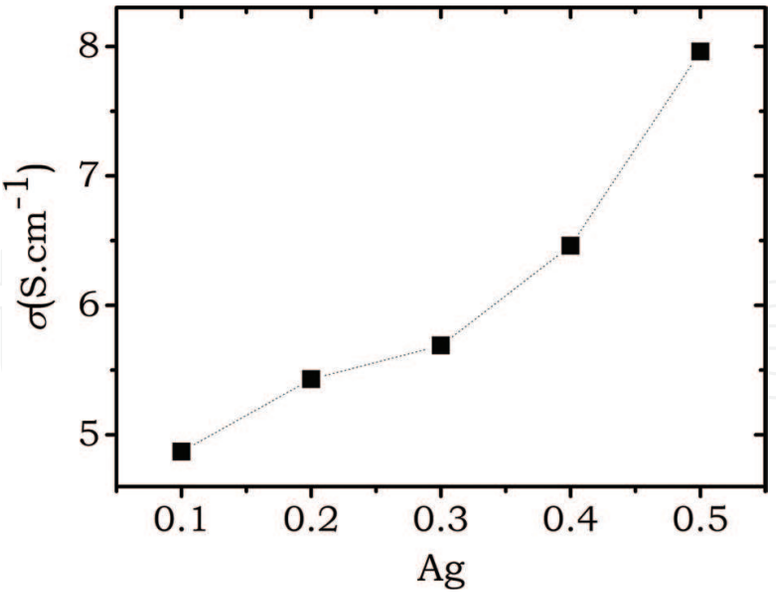

Figure 5. The influence of AgNPs on electrical conductivity of PANI.

result is comparable with the works reported by Wankhede et al. [44]. Unfortunately, they reported only for one composition of PANI-AgNPs, at various temperatures. Our results are far higher than that of PANI/PS/AgNPs nanocomposite samples [45].

The stability of electrical conductivity to PANI and AgNP composites were measured under the influence of ultrasonic irradiation. The various irradiation time was employed to the mixture of PANI-EB-AgNP solution prior to the deposition process. The electrical conductivity measurements of dwelling time are depicted in **Figure 6**.

It shows that the electrical conductivity of PANI-AgNP film has the stability of electrical conductivity values in the range 0.5–0.7 $S.cm^{-1}$. Out of that range, the duration of irradiation time

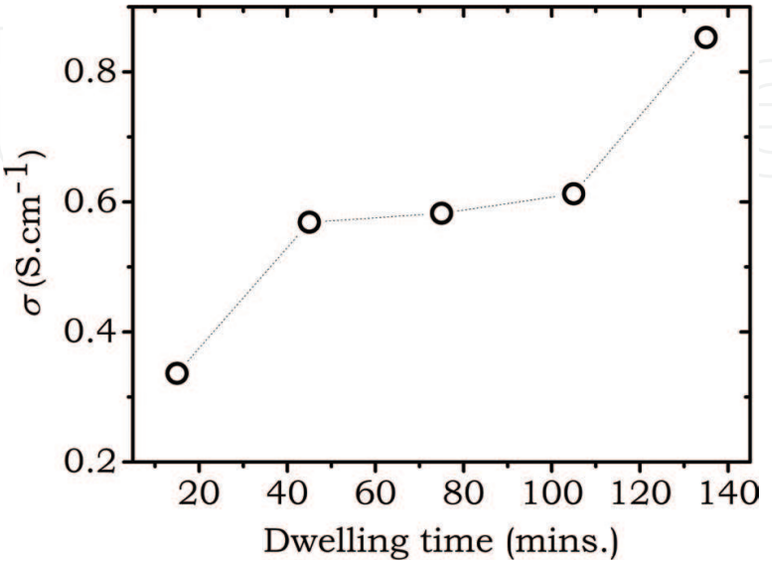

Figure 6. The stability electrical conductivity of PANI-AgNPs under ultrasonic irradiation.

is followed. It suggests that the intrinsic structure may also be changed by the ultrasonic irradiation dwelling time.

3.3. The influence of AgNPs on crystal size and conductivity of JML and PIW

Flavonoids of JML [46, 47] or PIW [48] are potential for the conductive organic polymer. Initially, the conductive polymer is in/below the semiconductor range after oxidizing or reducing process [49]. Also, the general polymer has an amorphous phase. When flavonoids extracted from JML are composited with AgNPs, we may expect that its electrical conductivity will increase. Here, we report the results of electrical conductivity measurement of AgNPs doped of JML and PIW flavonoids extracts. The crystallinity of the sample may be affected by the electrical conductivity, **Figure 7**. It indicates that the crystallinity of the sample increases with the increase of AgNP concentration in the composite.

As indicated in **Figure 7**, it is seen that the feature of AgNPs vs. crystallinity is not a linear, simple relationship. It shows a significant change in the range of 0.2–0.4 M of AgNPs, while substantial difference above or below that range. To look further, we plot the relation between AgNP concentration to its electrical conductivity, as shown in **Figure 8**.

The electrical conductivity of extracted JML flavonoid-AgNPs exponentially increases as the AgNPs increase. By comparing **Figure 8** with **Figure 7**, it is found that the rise in electrical conductivity does not merely support its crystallinity. It means that there is no direct or simple relationship.

AgNP-doped PIW flavonoid may show a similar feature. Roughly speaking, the role of AgNPs induced in the flavonoids' PIW-AgNP film also increases its crystallinity, as shown in **Figure 9**.

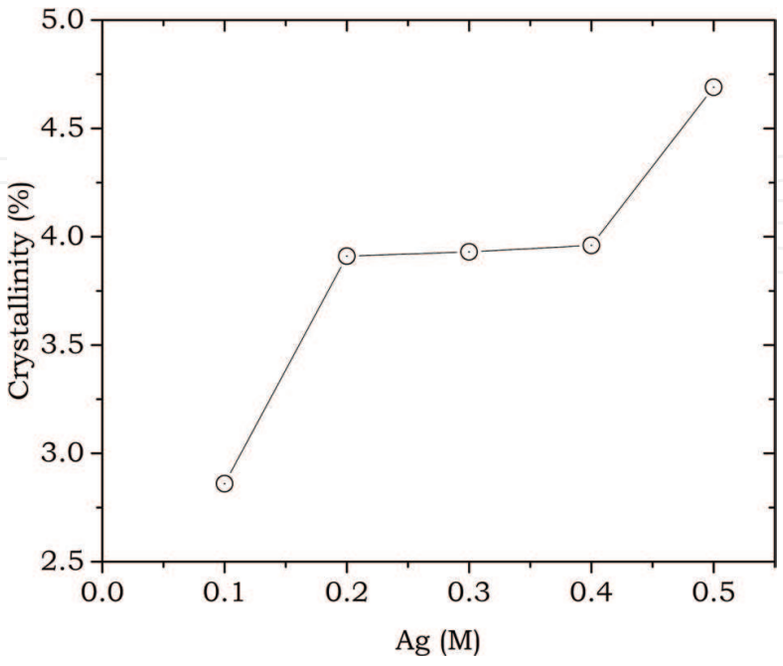

Figure 7. The influence of AgNPs on crystallinity JML.

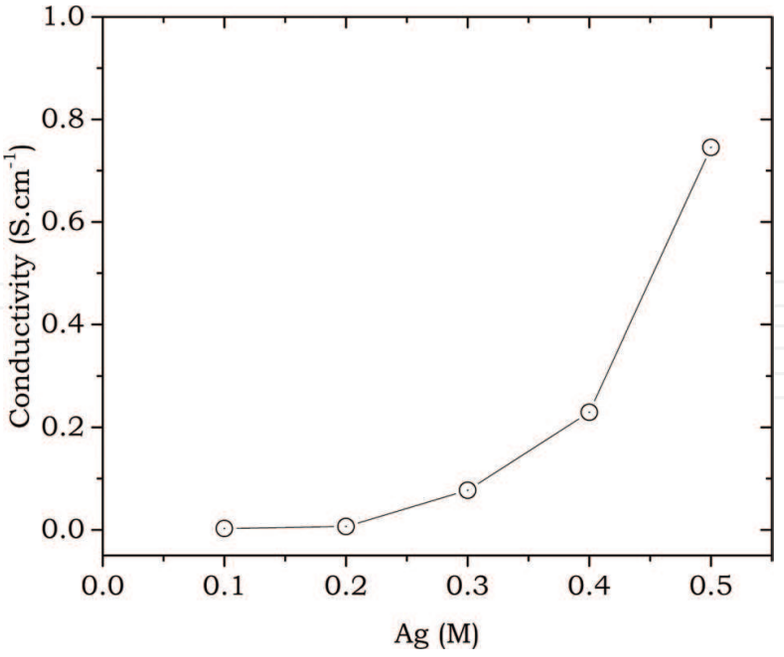

Figure 8. The influence of AgNPs on film JML-AgNPs.

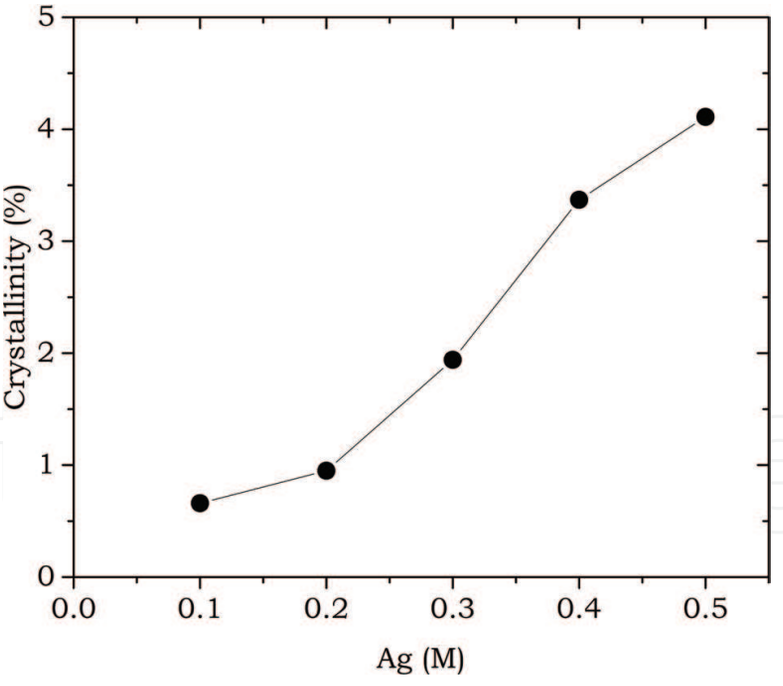

Figure 9. The influence of AgNPs on crystallinity flavonoid's PIW-AgNP film.

It is similar to its increase of crystallinity, the electrical conductivity of flavonoid's PIW-AgNP film is also increased as the increase of AgNPs, as illustrated in **Figure 10**.

By comparing **Figures 9** and **10**, it can be inferred that its crystallinity may characterize the increase of electrical conductivity of flavonoid's PIW-AgNP film. In another words, the role of AgNPs on the electrical conductivity of flavonoid's PIW-AgNP film is reflected by its

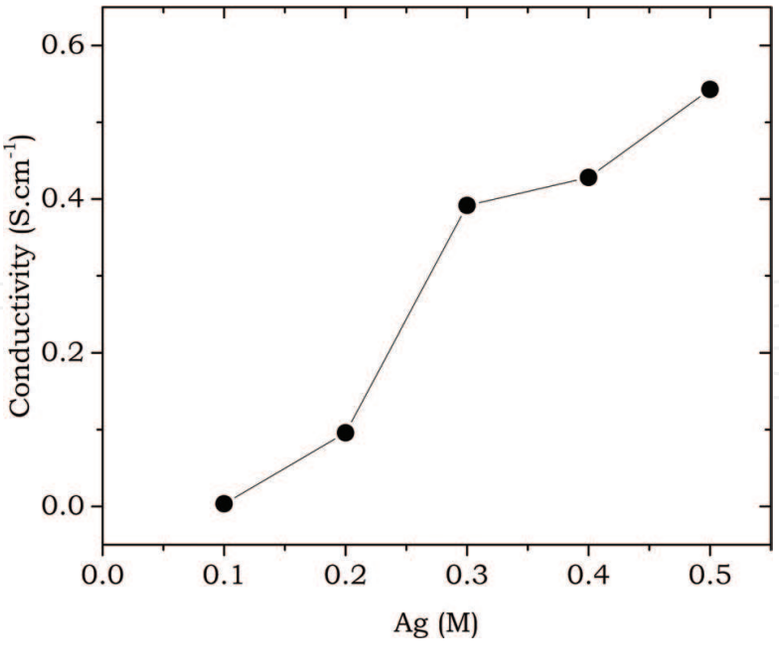

Figure 10. The influence of AgNPs on electrical conductivity of flavonoid's PIW-AgNP film.

crystallinity. As the electrical conductivity of flavonoids of PIW and JML shows different features, the type of flavonoid of both plants is possibly different. It is also possible that technically the distribution, or where the AgNPs interreact with, is also different.

Study of the role of AgNPs and polymers has been widely reported for many routes of synthesis and their applications [45, 50, 51]. Recently, AgNPs containing nanostructure nanocomposite have also been investigated for supercapacitors [52], polymer solar cells [53], or thin film silver-TiO_2 thermoelectric [54].

4. Conclusion

Some factors are influencing the size and the conductivity of AgNPs, i.e., the MSA concentration, ultrasonic irradiation time, as well as the concentration of PEG. In general, the increase of AgNP concentration gives rise to an increase in its electrical conductivity. Although the conductivity of polymers depends on AgNP concentration, the conductivity of the AgNPs doped of polymers does not directly reflect its crystallinity or crystal size.

AgNPs have excellent potential applications in medical, environment, electronics, dielectrics, and optical solar cell application. It is urgently required to perform an extensive research of various AgNPs and its derivatives for multiple applications.

Acknowledgements

The author thanks the Ministry of Research and Higher Education for the Research grants of University Excellent Research Grants, HUPT 2016, 2017, Primary Individual National Innovative Research Grant INSINAS 2017.

Author details

Markus Diantoro[1,2]*, Thathit Suprayogi[1], Ulwiyatus Sa'adah[1], Nandang Mufti[1,2], Abdulloh Fuad[1,2], Arif Hidayat[1] and Hadi Nur[3]

*Address all correspondence to: markus.diantoro.fmipa@um.ac.id

1 Department of Physics, Faculty of Mathematics and Natural Sciences, Universitas Negeri Malang, Malang, Indonesia

2 Center Laboratory for Minerals and Advanced Materials, Faculty of Mathematics and Natural Sciences, Universitas Negeri Malang, Malang, Indonesia

3 Centre for Sustainable Nanomaterials, Ibnu Sina Institute for Scientific and Industrial Research, Universiti Teknologi Malaysia, Skudai, Johor, Malaysia

References

[1] Lide DR. CRC Handbook of Chemistry and Physics: A Ready-Reference Book of Chemical and Physical Data. New York: CRC Press; 2008

[2] Ma R, Kang B, Cho S, Choi M, Baik S. Extraordinarily high conductivity of stretchable fibers of polyurethane and silver nanoflowers. ACS Nano. 2015;**9**:10876-10886. DOI: 10.1021/acsnano.5b03864

[3] Basak D, Karan S, Mallik B. Significant modifications in the electrical properties of poly(methyl methacrylate) thin films upon dispersion of silver nanoparticles. Solid State Communications. 2007;**141**:483-487. DOI: 10.1016/J.SSC.2006.12.014

[4] Gupta K, Jana PC, Meikap AK. Optical and electrical transport properties of polyaniline–silver nanocomposite. Synthetic Metals. 2010;**160**:1566-1573. DOI: 10.1016/J.SYNTHMET.2010.05.026

[5] Suganuma K, Sakamoto S, Kagami N, Wakuda D. Low-temperature low-pressure die attach with hybrid silver particle paste. Microelectronics. 2012;**52**:375-380

[6] Faddoul R, Reverdy-Bruas N, Blayo A, Haas T, Zeilmann C. Optimisation of silver paste for flexography printing on LTCC substrate. Microelectronics and Reliability. 2012;**52**:1483-1491. DOI: 10.1016/J.MICROREL.2012.03.004

[7] Bhattarai B, Chakraborty I, Conn BE, Atnagulov A, Pradeep T, Bigioni TP. High-yield paste-based synthesis of thiolate-protected silver nanoparticles. Journal of Physical Chemistry C. 2017;**121**:10964-10970. DOI: 10.1021/acs.jpcc.6b12427

[8] Diantoro M, Tjia MO, Kováč P, Hušek I. Pinning mechanisms in Bi-2223 tapes with reinforced Ag sheath and oxide additives in the core. Physica C: Superconductivity and Its Applications. 2001;**357-360**:1182-1185

[9] Kovác P, Husek I, Pachla W, Diantoro M, Bonfait G, Maria J, Fröhlich K, Kopera L, Diduszko R, Presz A. Material for resistive barriers in Bi-2223/Ag tapes. Superconductor Science and Technology. 2001;**14**:966-972. DOI: 10.1088/0953-2048/14/11/313

[10] Diantoro M, Loeksmanto W, Tjia M, Gömöry F, Šouc J, Hušek I, Kováč P. AC loss and critical current density in Bi-2223 tapes with oxide additives and reinforced Ag sheaths. Physica C: Superconductivity. 2002;**378-381**:1143-1147. DOI: 10.1016/S0921-4534(02)01728-8

[11] Oemry F, Diantoro M, Sutjahja IM, Tjia MO, Kopera L, Bonfait GMJ, Kovac P. Variation of vortex structure characteristics of Bi-2223/Ag superconducting tapes with respect to applied magnetic field direction. Physica C: Superconductivity. 2005;**426-431**:396-401. DOI: 10.1016/J.PHYSC.2005.02.051

[12] Jabur AR. B2223 high-temperature superconductor wires in silver sheath, filament diameter effect on critical temperature and current density. Energy Procedia. 2012;**18**:254-264. DOI: 10.1016/j.egypro.2012.05.037

[13] Rosarin FS, Mirunalini S. Nobel metallic nanoparticles with novel biomedical properties. Journal of Bioanalysis & Biomedicine. 2011;**3**:085-091. DOI: 10.4172/1948-593X.1000049

[14] Szczepanowicz K, Joanna S, Robert PS, Piotr W. Preparation of silver nanoparticles via chemical reduction and their antimicrobial activity. Physicochemical Problems of Mineral Processing. 2010;**45**:85-98

[15] Zhou W, Jia Z, Xiong P, Yan J, Li Y, Li M, Cheng Y, Zheng Y. Bioinspired, and biomimetic AgNPs/gentamicin-embedded silk fibroin coatings for robust antibacterial and osteogenetic applications. ACS Applied Materials & Interfaces. 2017;**9**:25830-25846. DOI: 10.1021/acsami.7b06757

[16] Dai X, Guo Q, Zhao Y, Zhang P, Zhang T, Zhang X, Li C. Functional silver nanoparticle as a benign antimicrobial agent that eradicates antibiotic-resistant bacteria and promotes wound healing. ACS Applied Materials & Interfaces. 2016;**8**:25798-25807. DOI: 10.1021/acsami.6b09267

[17] Leelavathi A, Bhaskara Rao T, Pradeep T. Supported quantum clusters of silver as enhanced catalysts for reduction. Nanoscale Research Letters. 2011;**6**:123. DOI: 10.1186/1556-276X-6-123

[18] Liang H, Wang W, Huang Y, Zhang S, Wei H. Controlled Synthesis of Uniform Silver Nanospheres. The Journal of Physical Chemistry C. 2010;**114**:7427-7431. DOI: 10.1021/jp9105713

[19] Zhang H, Duan T, Zhu W, Yao WT. Natural chrysotile-based nanowires decorated with monodispersed Ag nanoparticles as a highly active and reusable hydrogenation catalyst. Journal of Physical Chemistry C. 2015;**119**:21465-21472. DOI: 10.1021/acs.jpcc.5b05450

[20] Sarkar AK, Saha A, Midya L, Banerjee C, Mandre N, Panda AB, Pal S. Cross-linked biopolymer stabilized exfoliated titanate nanosheet-supported AgNPs: A green, sustainable

ternary nanocomposite hydrogel for catalytic and antimicrobial activity. ACS Sustainable Chemistry & Engineering. 2017;**5**:1881-1891. DOI: 10.1021/acssuschemeng.6b02594

[21] Elzey S, Grassian VH. Agglomeration, isolation and dissolution of commercially manufactured silver nanoparticles in aqueous environments. Journal of Nanoparticle Research. 2010;**12**:1945-1958. DOI: 10.1007/s11051-009-9783-y

[22] Purushotham E, Krishna NG. Preparation, and characterization of silver nanoparticles. Indian Journal of Physics. 2014;**88**:157-163. DOI: 10.1007/s12648-013-0396-z

[23] Reyes PY, Espinoza JA, Treviño ME, Saade H, López RG. Synthesis of silver nanoparticles by precipitation in bicontinuous microemulsions. Journal of Nanomaterials. 2010;**2010**:1-7. DOI: 10.1155/2010/948941

[24] Koski KJ, Kamp NM, Smith RK, Kunz M, Knight JK, Alivisatos AP. Structural distortions in 5-10 nm silver nanoparticles under high pressure. Physical Review B. 2008;**78**:165410. DOI: 10.1103/PhysRevB.78.165410

[25] Bahadory M. Synthesis of Noble Metal Nanoparticles. Pennsylvania: Drexel University; 2008 (Doctoral Thesis)

[26] Song KC, Lee SM, Park TS, Lee BS. Preparation of colloidal silver nanoparticles by chemical reduction method. Korean Journal of Chemical Engineering. 2009;**26**:153-155. DOI: 10.1007/s11814-009-0024-y

[27] Zielińska A, Skwarek E, Zaleska A, Gazda M, Hupka J. Preparation of silver nanoparticles with controlled particle size. Procedia Chemistry. 2009;**1**:1560-1566. DOI: 10.1016/J.PROCHE.2009.11.004

[28] Malekzadeh M, Halali M. Method of producing high purity silver nanoparticles. 2012. No. US 20120060649A1

[29] Esfahani NN, Toghraie D, Afrand M. A new correlation for predicting the thermal conductivity of ZnO–Ag (50%–50%)/water hybrid nanofluid: An experimental study. Powder Technology. 2018;**323**:367-373. DOI: 10.1016/J.POWTEC.2017.10.025

[30] Meng Y, Su F, Chen Y. Effective lubricant additive of nano-Ag/MWCNTs nanocomposite produced by supercritical CO_2 synthesis. Tribology International. 2018;**118**:180-188. DOI: 10.1016/J.TRIBOINT.2017.09.037

[31] Tan M, Wang X, Hao Y, Deng Y. Novel Ag nanowire array with high electrical conductivity and fast heat transfer behavior as the electrode for film devices. Journal of Alloys and Compounds. 2017;**701**:49-54. DOI: 10.1016/J.JALLCOM.2017.01.086

[32] Anandhakumar S, Sasidharan M, Tsao C-W, Raichur AM. Tailor-made hollow silver nanoparticle cages assembled with silver nanoparticles: An efficient catalyst for epoxidation. ACS Applied Materials & Interfaces. 2014;**6**:3275-3281. DOI: 10.1021/am500229v

[33] Liu J, Hurt RH. Ion release kinetics and particle persistence in aqueous nano-silver colloids. Environmental Science & Technology. 2010;**44**:2169-2175. DOI: 10.1021/es9035557

[34] Ghosale A, Shankar R, Ganesan V, Shrivas K. Direct-writing of paper based conductive track using silver nano-ink for electroanalytical application. Electrochimica Acta. 2016;**209**:511-520. DOI: 10.1016/J.ELECTACTA.2016.05.109

[35] Diantoro M, Fitrianingsih R, Mufti N, Fuad A. Synthesis of silver nanoparticles by chemical reduction at various fraction of MSA and their structure characterization. In: AIP Conference Proceedings; 2014. pp. 257-261. DOI: 10.1063/1.4868795

[36] Majeed Khan MA, Kumar S, Ahamed M, Alrokayan SA, AlSalhi M. Structural and thermal studies of silver nanoparticles and electrical transport study of their thin films. Nanoscale Research Letters. 2011;**6**:434. DOI: 10.1186/1556-276X-6-434

[37] Shameli K, Bin Ahmad M, Jazayeri SD, Sedaghat S, Shabanzadeh P, Jahangirian H, Mahdavi M, Abdollahi Y. Synthesis and characterization of polyethylene glycol mediated silver nanoparticles by the green method. International Journal of Molecular Sciences. 2012;**13**:6639-6650. DOI: 10.3390/ijms13066639

[38] Lu YC, Sen Chou K. A simple and effective route for the synthesis of nano-silver colloidal dispersions. Journal of the Chinese Institute of Chemical Engineers. 2008;**39**:673-678. DOI: 10.1016/j.jcice.2008.06.005

[39] Larson A, Von Dreele R. General Structure Analysis System. New Mexico: Los Alamos; 1994

[40] Rodriguez-Carvajal J, Roisnel T. FullProf-Manual. Grenoble, France: Institute Laue-Langevin; 1992

[41] Mishra S, Shimpi NG, Sen T. The effect of PEG encapsulated silver nanoparticles on the thermal and electrical property of sonochemically synthesized polyaniline/silver nanocomposite. Journal of Polymer Research. 2013;**20**:49. DOI: 10.1007/s10965-012-0049-5

[42] Abou El-Nour KMM, Eftaiha A, Al-Warthan A, Ammar RAA. Synthesis and applications of silver nanoparticles. Arabian Journal of Chemistry. 2010;**3**:135-140. DOI: 10.1016/j.arabjc.2010.04.008

[43] Mansouri SS, Ghader S. Experimental study on effect of different parameters on size and shape of triangular silver nanoparticles prepared by a simple and rapid method in aqueous solution. Arabian Journal of Chemistry. 2009;**2**:47-53. DOI: 10.1016/j.arabjc.2009.07.004

[44] Wankhede YB, Kondawar SB, Thakare SR, More PS. Synthesis and characterization of silver nanoparticles embedded in polyaniline nanocomposite. Advanced Materials Letters. 2013;**4**:89-93. DOI: 10.5185/amlett.2013.icnano.108

[45] Youssef AM, Mohamed SA, Abdel-Aziz MS, Abdel-Aziz ME, Turky G, Kamel S. Biological studies and electrical conductivity of paper sheet based on PANI/PS/Ag-NPs nanocomposite. Carbohydrate Polymers. 2016;**147**:333-343. DOI: 10.1016/J.CARBPOL.2016.03.085

[46] Falodun A, Imieje V, Erharuyi O, Joy A, Langer P, Jacob M, Khan S, Abaldry M, Hamann M. Isolation of antileishmanial, antimalarial and antimicrobial metabolites from *Jatropha multifida*. Asian Pacific Journal of Tropical Biomedicine. 2014;**4**:374-378. DOI: 10.12980/APJTB.4.2014C1312

[47] Rampadarath S, Puchooa D, Ranghoo-Sanmukhiya VM. Antimicrobial, phytochemical and larvicidal properties of *Jatropha multifida* Linn. Asian Pacific Journal of Tropical Medicine. 2014;**7**:S380-S383. DOI: 10.1016/S1995-7645(14)60262-5

[48] Khan MR, Omoloso AD. Antibacterial activity of *Pterocarpus indicus*. Fitoterapia. 2003;**74**: 603-605. DOI: 10.1016/S0367-326X(03)00149-7

[49] Lange U, Roznyatovskaya NV, Mirsky VM. Conducting polymers in chemical sensors and arrays. Analytica Chimica Acta. 2008;**614**:1-26. DOI: 10.1016/j.aca.2008.02.068

[50] Ragachev AA, Yarmolenko MA, Xiaohong J, Shen R, Luchnikov PA, Rogachev AV. Molecular structure, optical, electrical and sensing properties of PANI-based coatings with silver nanoparticles deposited from the active gas phase. Applied Surface Science. 2015;**351**:811-818. DOI: 10.1016/j.apsusc.2015.06.008

[51] Abbasi NM, Yu H, Wang L, Zain-Ul-Abdin, Amer WA, Akram M, Khalid H, Chen Y, Saleem M, Sun R, Shan J. Preparation of silver nanowires and their application in conducting polymer nanocomposites. Materials Chemistry and Physics. 2015;**166**:1-15. DOI: 10.1016/j.matchemphys.2015.08.056

[52] Luo S, Yu S, Sun R, Wong CP. Nano Ag-deposited $BaTiO_3$ hybrid particles as fillers for polymeric dielectric composites: Toward high dielectric constant and suppressed loss. ACS Applied Materials & Interfaces. 2014;**6**:176-182. DOI: 10.1021/am404556c

[53] Tran QT, Thu HT, Tran VS, Cuong TV, Hong C. Solution-processed rGO/AgNPs/rGO sandwich structure as a hole extraction layer for polymer solar cells. Materials (Basel). Journal of Materials. 2015;**2015**:1-5. DOI: 10.1155/2015/652645

[54] Jung SY, Ha TJ, Park CS, Seo WS, Lim YS, Shin S, Cho HH, Park HH. Improvement in the conductivity ratio of ordered mesoporous Ag-TiO_2 thin films for thermoelectric materials. Thin Solid Films. 2013;**529**:94-97. DOI: 10.1016/j.tsf.2012.03.087